

X-ray nano computerised tomography of SOFC electrodes using a focused ion beam sample-preparation technique

P.R. Shearing^{a,*}, J. Gelb^b, N.P. Brandon^a

^a Department of Earth Science and Engineering, Imperial College, London, UK

^b Xradia Inc., 5052 Commercial Circle, Concord, CA 94520, USA

Received 18 August 2009; received in revised form 26 January 2010; accepted 3 February 2010

Available online 4 March 2010

Abstract

High-resolution tomography techniques have facilitated an improved understanding of solid oxide fuel cell (SOFC) electrode microstructures.

The use of X-ray nano computerised tomography (nano-CT) imposes some geometrical constraints on the sample under investigation; in this paper, we present the development of an advanced preparation technique to optimise sample geometries for X-ray nano-CT, utilizing a focused ion beam (FIB) system to shape the sample according to the X-ray field of view at the required magnification.

The technique has been successfully applied to a Ni-YSZ electrode material: X-ray nano-CT has been conducted at varying length scales and is shown to provide good agreement; comparison of results from X-ray and more conventional FIB tomography is also demonstrated to be favourable.

Tomographic reconstructions of SOFC electrodes with volumes spanning two orders of magnitude are presented.

© 2010 Elsevier Ltd. All rights reserved.

Keywords: Fuel cells; X-ray methods; Microstructure; Focused ion beam; SOFC

1. Introduction

Solid Oxide Fuel Cells (SOFCs) are high-temperature electrochemical energy-conversion devices with the potential for economic power generation at high efficiency and with significantly reduced emissions. SOFCs are centred on a redox reaction, in which hydrogen (and also carbon monoxide, if present) is oxidised at the anode and oxygen is reduced at the cathode; the resulting external current flow generates useful electrical energy. Porous electrodes are used to support the redox reactions at both anode and cathode. A common choice for anode materials is the porous composite Ni-YSZ (Yttria Stabilised Zirconia) because of its low-cost, thermal and chemical stability, electronic conductivity, and catalytic activity for hydrogen oxidation.¹

In common with all functional materials, the microstructure of SOFC electrodes has a direct influence on its performance, affecting the electrical, electrochemical, diffusion, and mechanical performance of the electrode. The importance of electrode

microstructure is widely acknowledged (see e.g.²) and electrode design and manufacture remains an important barrier to the successful commercialisation of SOFC technology. However, there remains little agreement as to what constitutes a “good” microstructure.³ Attempts to infer improvements in microstructure by the study of secondary factors are often inconclusive; therefore, any technique that can be used to provide direct, quantitative information on electrode microstructure is highly valuable.

Traditionally, the resolution limits of conventional X-ray computed tomography have limited its application for the study of SOFC electrodes which characteristically have sub-micron feature sizes. However, the introduction of nano-scale CT systems has facilitated the use of X-ray techniques alongside the higher resolution dual-beam FIB-SEM (focused ion beam-scanning electron microscope) tomography^{4–6} for the study of SOFC electrode microstructures in three dimensions.

Implementation of X-ray optics have been largely responsible for the improvements in the resolution of X-ray CT observed in recent years.⁷ Fig. 1 shows the set-up of a typical X-ray nano-CT system which utilizes a dual-lens system to focus the incident and transmitted X-ray beams. Analogous to other transmission-based microscopes, resolution is defined primarily

* Corresponding author. Tel.: +44 20 75949981.

E-mail address: p.shearing@imperial.ac.uk (P.R. Shearing).

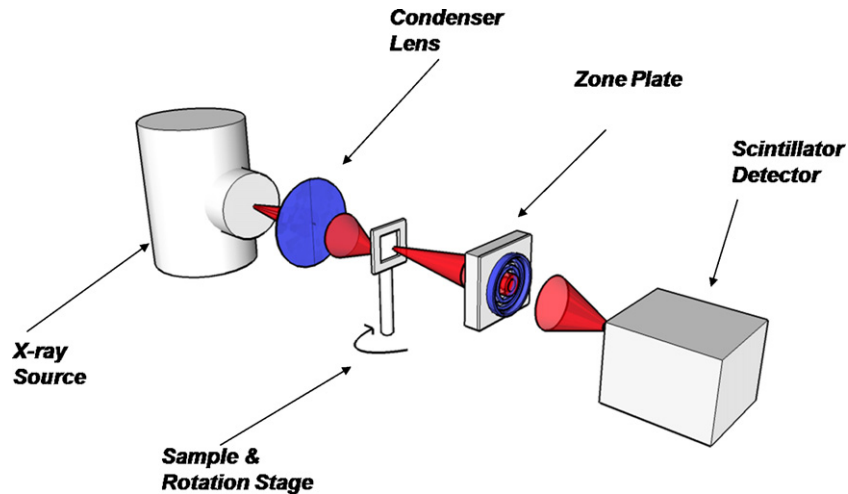


Fig. 1. Schematic diagram of a lens-based X-ray nano-CT system; the system utilizes X-ray optics to focus the incident and transmitted beam enabling high-resolution 3D X-ray CT imaging.

by the parameters of the lenses, enabling resolution down to 10 s of nanometres. Due to the non-destructive nature of X-ray imaging, the sample remains intact for further analysis, providing some significant advantages over traditional imaging techniques.

In CT scans with a parallel-beam configuration, the sample is rotated through 180° relative to the X-ray source with projection micrographs collected at discrete angular steps; the data can then be reconstructed using standard parallel-beam back projection algorithms to produce a 3D volume.⁸ In order to maximise the quality of the reconstruction, the sample geometry should correspond to the field of view at the required magnification, ensuring that the sample is completely contained throughout its rotation. This requires the use of precision sample-preparation equipment prior to imaging; one such technique using FIB lift-out will be described later in more detail.

The dimensions of non-uniform geometries can be described by a number of characteristic dimensions. The Greatest Feret Diameter (d_{gf} , also known as the least bounding circle dimension) of a particle is defined as the largest distance between two parallel lines that do not intersect the particle⁹ and is shown in Fig. 2a. To optimise the quality of tomographic data, the Greatest Feret Diameter of the particle in the plane of the transmitted X-ray defines the minimum FOV that should be used; this is shown schematically in Fig. 2b.

If the region of interest is not maintained within the FOV for the full rotation, the algorithm must essentially reconstruct an incomplete data set; ultimately, this increases the noise observed in the reconstruction. Furthermore, in tomographic studies of composite materials; phase identification is typically achieved by observation of the spatial distribution of X-ray absorption. However, if the sample is not maintained within the X-ray FOV throughout the rotation, the attenuation due to sample geometry and that due to material composition cannot be isolated leading to challenges in reconstructing the difference phases within large specimens. Banhart¹⁰ provides further discussion of this limitation due to “missing data”.

The Xradia nanoXCT-100 laboratory scanner was used in this study, utilizing both available magnifications of $200\times$ and $800\times$

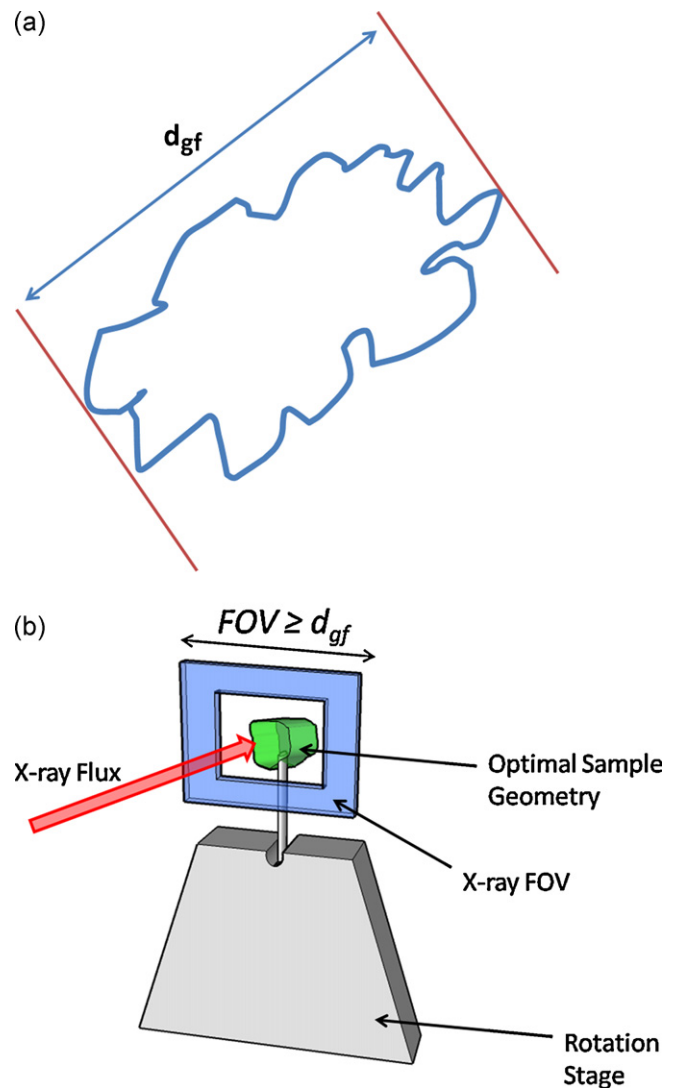


Fig. 2. a) Greatest Feret Diameter of a non-uniform particle. b) An optimal sample geometry should ensure that the sample is maintained in the X-ray FOV throughout the rotation (i.e. $FOV \geq d_{gf}$).

(15 and 60 μm FOV, respectively). In order to optimise sample geometry for the nano-scale CT, an advanced lift-out procedure for sample preparation was developed.

Here, we present the development and application of X-ray nano-CT imaging utilizing FIB lift-out sample preparation for the characterisation of Ni-YSZ materials with variable magnification. In order to validate the X-ray measurements, results are compared with a reconstruction obtained using dual-beam FIB-SEM, from which good correlation is observed.

2. Experimental

NiO-YSZ powder (66 wt% NiO, 34 wt% YSZ) was supplied by Nextech Fuel Cell Materials. The powder was pressed into pellet form under 1 tonne of pressure before sintering at 1350 °C for 12 h. The resulting pellets were reduced in H_2 at 900 °C for 4 h with reduction conditions sufficiently rigorous to ensure all of the NiO was reduced. The resulting Ni-YSZ microstructure was characterised using X-ray nano-CT, both with 200 \times and 800 \times total magnification. The former magnification provided a FOV of 60 μm \times 60 μm with spatial resolution of ca. 200 nm and the latter a FOV of 15 μm \times 15 μm with spatial resolution of ca. 50 nm.^{11,12}

In order to maximise the quality of the 3D rendering, a novel sample-preparation technique has been adopted. The sample-preparation technique used a focused ion beam to prepare an

optimal geometry for high-resolution nano-CT based on lift-out and ex situ processing. FIB lift-out was conducted using single ion beam equipment (FEI FIB200). The process is outlined in Fig. 3.

The focused ion beam was used to first mill around an area of interest, isolating a material micro-section secured to the bulk sample by a small connecting bridge (Fig. 3a). A micro-manipulator needle was introduced (Kleindiek Nanotechnik MM3-EM) and then welded to the micro-section using a Pt gas injection system, common to most FIB systems.¹³ With the micro-manipulator securely welded, the connecting bridge was detached by ion beam milling and the micro-section removed from the electrode bulk (Fig. 3c). The sample mounted on the tungsten needle was then particularly well-suited for X-ray CT imaging due to its small form factor, allowing for full 180° rotation within the working distances of the nano-CT instrument. Fig. 3d shows an X-ray transmission micrograph of the sample welded onto the end of the micro-manipulator needle and Fig. 3e shows the sample inserted into the instrument's sample holder. This sample-preparation technique also allows site-specific sample preparation as well as the ability to perform shaping of the sample geometry to provide rotationally symmetrical samples if required.

For collection of tomography data, the sample was rotated through 180° with X-ray projection images collected at discrete angular steps. Using 200 \times magnification, images were

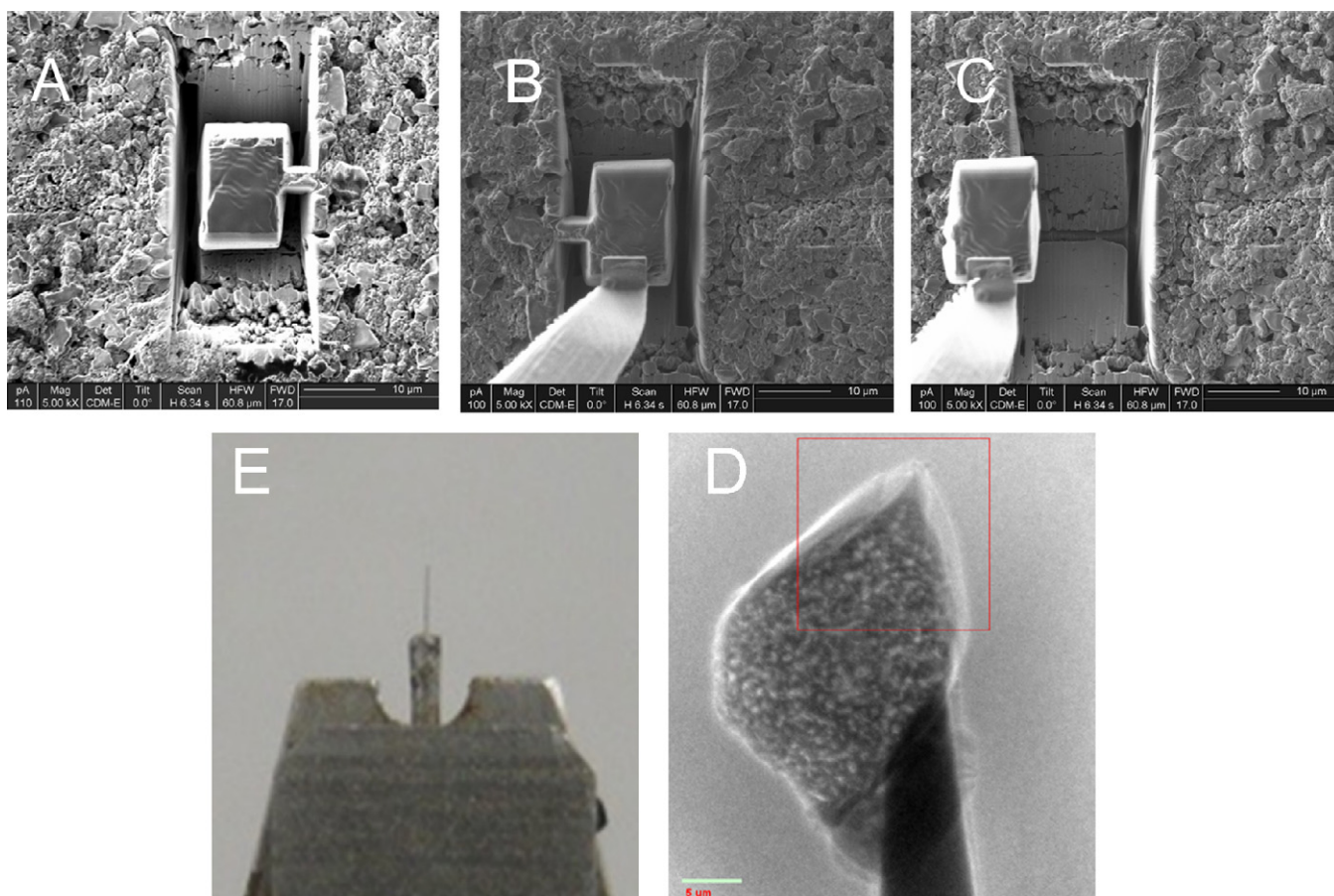


Fig. 3. a–c) FIB lift-out procedure for preparation of X-ray sample. d) X-ray transmission micrograph of sample. e) Sample inserted in X-ray sample holder.

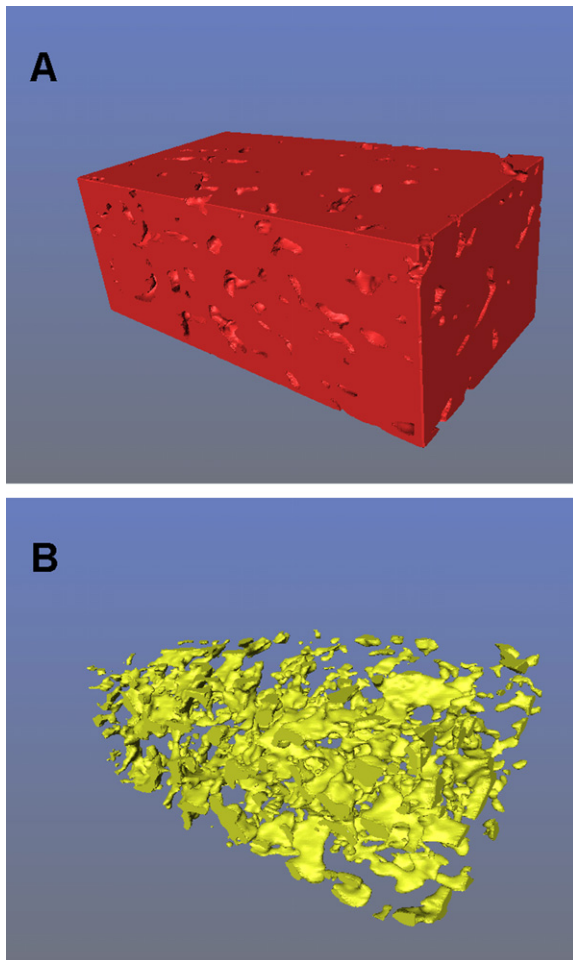


Fig. 4. a) Solid phase reconstruction. b) Pore phase reconstruction (reconstructed volume = $11.78 \mu\text{m} \times 6.27 \mu\text{m} \times 4.48 \mu\text{m}$).

collected at steps of 0.2° across 180° total rotation using a 1024×1024 pixel Peltier-cooled CCD detector; using $800\times$ magnification, angular steps of 0.6° were used across the same range and with the same detection system. The virtual 3D volume was formed from the projection images by employing a standard parallel-beam filtered back-projection algorithm.

3. Results and discussion

A lift-out sample has been prepared using the techniques outlined above and investigated with X-ray tomography using two different levels of magnification:

Using the nano-CT in its highest resolution configuration, a sample volume of $11.78 \mu\text{m} \times 6.27 \mu\text{m} \times 4.48 \mu\text{m}$ was reconstructed with a voxel size of $32 \text{ nm} \times 32 \text{ nm} \times 32 \text{ nm}$ (down sampling pre-reconstruction by 2 times). The rendering of the solid phase is shown in Fig. 4a, and that of the pore phase is shown in Fig. 4b.

In the lower magnification mode, the total sample volume characterised was $37,945 \mu\text{m}^3$ with voxel dimensions of $65 \text{ nm} \times 65 \text{ nm} \times 65 \text{ nm}$. Fig. 5a shows an individual slice from the CT reconstruction; Fig. 5b–d show various renderings of the reconstructed volume.

Volume renderings and image analysis of both tomography sequences have been conducted using Amira visualisation and analysis software to segment the solid and pore phases. The improvements in raw image quality facilitate the use of standard image processing techniques with limited filtering, representing an advantage over FIB techniques where isolation of pore phases can require the use of complex algorithms¹⁴ or the use of resin impregnation.^{15,16}

In Fig. 5d, the colour distribution represents a variable optical density inside the sample; as the sample geometry is maintained within the X-ray FOV for the duration of the scan, these colour changes may be attributed to changes in composition. The blue areas are believed to correspond to pores and re-deposited materials from the sample-preparation procedure, green to Ni, and red to YSZ. Whilst differences in optical density are evident in both imaging modes, these have not been sufficiently uniform to allow segmentation of the individual solid phases. However, use of synchrotron radiation may afford improved phase contrast by manipulation of the X-ray energy around characteristic elemental edges.¹⁰

Microstructural data extracted from the nano-CT data is presented in Table 1. The results are compared with previously published data from FIB tomography obtained from the same pellet sample.

The measured porosity using X-ray nano-CT with $800\times$ magnification is 8.81% and, with $200\times$ magnification, the X-ray tomography predicts porosity of 9.25%. Both results are in broad agreement with the porosity measured by FIB techniques for a tomography sequence from the same electrode pellet sample (9.42%).⁵

The agreement in porosity measurements performed using both X-ray and FIB equipment provides experimental validation of the techniques. The results also demonstrate a significant advancement from conventional porosimetry techniques, as with knowledge of the three-dimensional pore distribution it is possible to extract useful geometrical parameters such as volume specific surface area, phase tortuosity and curvature.^{4,11,17}

The non-destructive nature of the X-ray nano-CT technique provides a significant advantage compared with destructive FIB techniques. Whilst comparison of electrode microstructures obtained using destructive imaging techniques provides valuable information, the representative volume element under consideration must account for local heterogeneities, thus providing purely statistical results. Furthermore, whilst attempts have been made to characterise the effects of time dependent microstructural changes using FIB techniques (e.g. study of Ni coarsening during long term operation^{18,19}), the extraction of kinetic parameters is intrinsically limited by statistical variations. The ability to characterise the same microstructure before and after change, without complications introduced by localised heterogeneities is therefore highly desirable.

The lift-out technique provides a robust sample for handling and transportation; the sample can also be routinely heated and exposed to varying gas environments, providing an ideal geometry for studies of microstructural evolution.

In this instance, it has not been possible to isolate triple phase contact reliably using the laboratory CT system. Char-

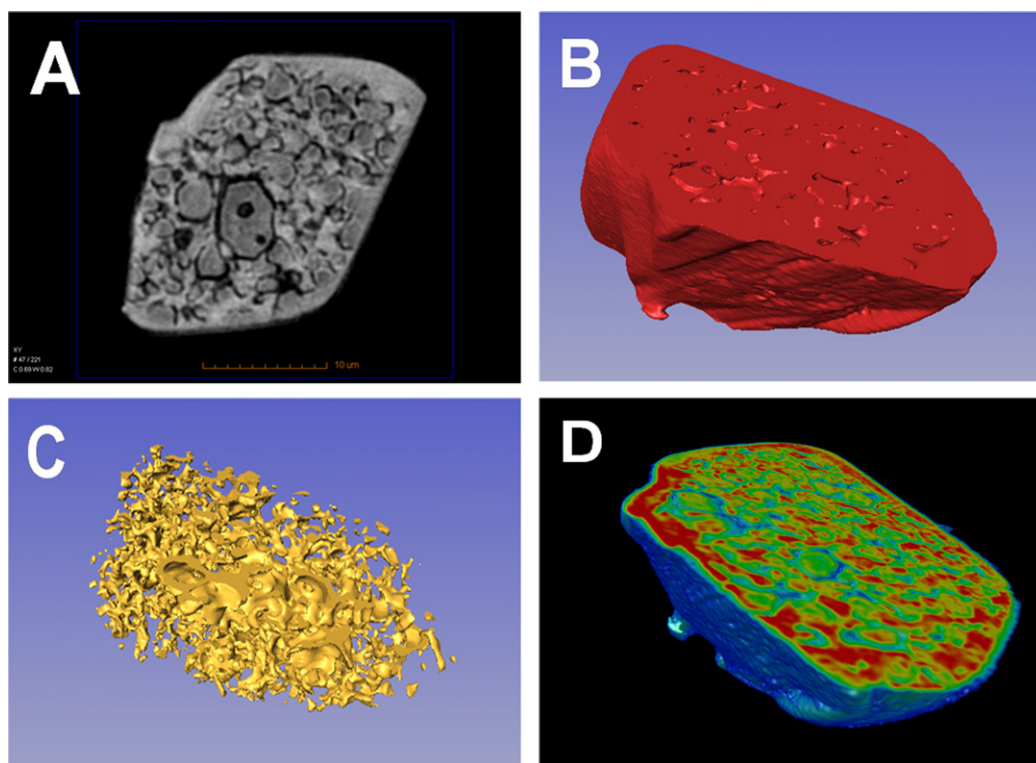


Fig. 5. a) Individual slice from large FOV nCT scan. b) Solid phase reconstruction. c) Pore phase reconstruction. d) 3D volume rendering showing changes in X-ray absorption (total volume of reconstruction $37,945 \mu\text{m}^3$). (For interpretation of the references to color in this figure legend, the reader is referred to the web version of the article.)

Table 1
Microstructural Information for FIB and X-ray tomography techniques.

Reconstruction	Voxel dimension (nm)			Reconstruction volume (μm)			Volume %			Percolated TPB density (μm^{-2})
	X	Y	Z	X	Y	Z	Ni	YSZ	Pore	
X-ray (small FOV)	32	32	32	11.78	6.27	4.48	91.19	8.81	–	
X-ray (large FOV)	65	65	65			$37945 \mu\text{m}^3$	90.75	9.25	–	
FIB	20	20	19	17.80	12.18	3.33	63.17	27.41	9.42	4.25

acteristic absorption changes have been identified, which highlights the potential for synchrotron-based experiments. In laboratory based systems, the potential for characterisation of three-dimensional pore distribution and single phase materials is compelling, for example the potential to interface the tomography data with diffusion simulations using the real-life microstructure as a framework. However, further experiments must be performed in order to make this approach practical.

Any tomography procedure must balance the dual requirements of providing sufficient resolution to identify characteristic microstructural features whilst also ensuring a sufficient sample volume is characterised to represent the bulk microstructure. The ability to conduct tomography over a variable FOV is therefore valuable. In this instance, the agreement between the data obtained in high resolution and large FOV configurations (and also with data from FIB tomography) suggests that characterisation of the material microstructures presented here with ca. 200 nm spatial resolution is sufficient. Furthermore, this demonstrates that a sacrifice in resolution can be coupled to an increase in reconstructed volume without compromising key

microstructural data. Here, we report successful characterisation of a sample volume of $37,945 \mu\text{m}^3$; at the time of writing, this is more than an order of magnitude larger than the largest FIB reconstruction known to the authors.¹⁵

Clearly, the resolution required is dependent on the individual microstructure under investigation and similar experiments would be required to optimise the balance of resolution and imaging volume on a case-by-case basis.

4. Conclusions

In this paper, an advanced FIB sample-preparation technique for X-ray computed tomography has been presented. The technique provides optimal geometries for nano-CT by ensuring the Greatest Feret Diameter is no larger than the X-ray FOV. The sample-preparation technique is also robust and site specific. Variable-volume X-ray nano-CT has been conducted and reconstructions of SOFC electrodes with volumes spanning two orders of magnitude were demonstrated.

X-ray and FIB-based tomographic analysis of samples from the same Ni-YSZ anode batch have shown good agreement which lends experimental validation of the techniques for complementary analysis of SOFC microstructures. In lab-based nano-CT systems, characteristic changes in X-ray absorption corresponding to chemical phase changes have been identified; whilst these have not provided sufficient uniformity for analysis of triple phase contact in these materials, they indicate the value of laboratory systems not only for characterisation of pore distribution or single phase materials but also as a pre-qualification experiment for synchrotron investigations.

The ability to provide quantitative analysis of electrode microstructures in 3D is of increasing importance to the fuel cell community. Advanced tomographic techniques afford access to key microstructural metrics including the distribution of material and pore phases in 3D, which not only allows direct comparison of electrode microstructures but also offers the ability to link microstructure with electrochemical performance. Furthermore, with the increasing maturity of these techniques, it should be possible to identify mechanisms of microstructural evolution through processing and environmental changes.

These techniques are by no means restricted to applications in fuel cell research and can be used for microstructural characterisation of a wide range of materials including structural and functional ceramics, catalyst supports and energy storage materials.

Acknowledgements

This work has been supported by the EPSRC Supergen fuel cells programme. The authors gratefully acknowledge the support of Xradia, Inc. for assistance with X-ray studies. The authors thank Michael Drakopolous, Wah-Keat Lee, and JaeMock Yi for many useful discussions. Finally, the authors wish to acknowledge EPSRC grant GR/T26344 for access to image processing software.

References

- Cheng Z, Wang J, Liu M. Anodes. In: Fergus JW, et al., editors. *Solid oxide fuel cells—materials properties and performance*. Boca Raton CRC Press; 2009.
- Brandon NP, Brett DJ. Engineering porous materials for fuel cell applications. *Philosophical Transactions of the Royal Society a-Mathematical Physical and Engineering Sciences* 2006;**364**(1838):147–59.
- Waldbillig D, Wood A, Ivey DG. Electrochemical and microstructural characterization of the redox tolerance of solid oxide fuel cell anodes. *Journal of Power Sources* 2005;**145**(2):206–15.
- Gostovic D, Smith JR, Kundinger DP, Jones KS, Wachsman ED. Three-dimensional reconstruction of porous LSCF cathodes. *Electrochemical and Solid State Letters* 2007;**10**(12):B214–7.
- Shearing PR, Golbert J, Chater RJ, Brandon NP. 3D reconstruction of SOFC anodes using a focused ion beam lift-out technique. *Chemical Engineering Science* 2009;**64**(17):3928–33.
- Wilson JR, Kobsiriphat W, Mendoza R, Chen HY, Hiller JM, Miller DJ, et al. Three-dimensional reconstruction of a solid-oxide fuel-cell anode. *Nature Materials* 2006;**5**(7):541–4.
- Withers PJ. X-ray nanotomography. *Materials Today* 2007;**10**(12):26–34.
- Natterer F, editor. *The mathematics of computerized tomography*. Chichester: John Wiley & Sons; 1986.
- Church T. Problems associated with the use of the ratio of Martin's diameter to Feret's diameter as a profile shape factor. *Powder Technology* 1968;**2**(1):27–31.
- Banhart J, editor. *Advanced tomographic methods in materials research and engineering*. Oxford: Oxford University Press; 2008.
- Izzo JR, Joshi AS, Grew KN, Chiu WKS, Tkachuk A, Wang SH, et al. Nondestructive reconstruction and analysis of SOFC anodes using x-ray computed tomography at sub-50 nm resolution. *Journal of the Electrochemical Society* 2008;**155**(5):B504–8.
- Feser M, Gelb J, Chang H, Cui H, Duewer F, Lau SH, et al. Sub-micron resolution CT for failure analysis and process development. *Measurement Science & Technology* 2008;**19**(9).
- Yao N, editor. *Focused ion beam system basics and applications*, vol. 395. Cambridge: Cambridge University Press; 2007.
- Jorgensen PS, Bowen JR. *Automatic quantitative image analysis of micrographs*. Lucerne: 8th European Fuel Cell Forum, EFCF; 2008.
- Iwai H, Shikazono N, Matsui T, Teshima H, Kishimoto M, Kishida R, et al. Quantification of SOFC anode microstructure based on dual beam FIB-SEM technique. *Journal of Power Sources* 2009;**195**(4):955–61.
- Ruger B, Joos J, Weber A, Carraro T, Iver-Tiffée E. *3D electrode microstructure reconstruction and modelling*. Vienna: SOFC-XI, ECS; 2009.
- Wilson JR, Cronin JS, Duong AT, Rukes S, Chen H-Y, Thornton K, et al. Effect of composition of (La_{0.8}Sr_{0.2}MnO₃-Y₂O₃-stabilized ZrO₂) cathodes: correlating three-dimensional microstructure and polarization resistance. *Journal of Power Sources* 2009;**195**(7):1829–40.
- Galinski H, Reuteler J, Rupp JLM, Bieberle-Hutter A, Gauckler LJ. *Ostwald ripening and oxidation kinetics of nickel gadolinia doped ceria anodes*. Vienna: SOFC-XI, ECS; 2009.
- Shearing PR. *Characterisation of SOFC electrode microstructures in three dimensions*. PhD thesis. London: Imperial College; 2009.